Evolution of the Bhandara-Balaghat granulite belt along the southern margin of the Sausar Mobile Belt of central India

H M Ramachandra[1] and Abhinaba Roy[2]

[1]*Geological Survey of India, AMSE Wing, Bangalore 560 078*
[2]*Geological Survey of India, Central Region, Nagpur 440 006*

The Bhandara-Balaghat granulite (BBG) belt occurs as a 190 km long, detached narrow, linear, NE–SW to ENE–WSW trending belt that is in tectonic contact on its northern margin with the Sausar Group of rocks and is bordered by the Sakoli fold belt in the south. The Bhandara part of the BBG belt is quite restricted, comprising a medium to coarse grained two-pyroxene granulite body that is of gabbroic composition and preserves relic igneous fabric. The main part of the belt in Arjuni-Balaghat section includes metasedimentary (quartzite, BIF, Al- and Mg-Al metapelites) and metaigneous (metaultramafic, amphibolite and two-pyroxene granulite) protoliths interbanded with charnockite and charnockitic gneiss. These rocks, occurring as small bands and enclaves within migmatitic and granitic gneisses, show polyphase deformation and metamorphism. Geochemically, basic compositions show tholeiitic trend without Fe-enrichment, non-komatitic nature, continental affinity and show evolved nature. Mineral parageneses and reaction textures in different rock compositions indicate early prograde, dehydration melt forming reactions followed by orthopyroxene stability with or without melt. Coronitic and symplectitic garnets have formed over earlier minerals indicating onset of retrograde IBC path. Evidences for high temperature ductile shearing are preserved at places. Retrogressive hydration events clearly post-date the above paths. The present study has shown that the BBG belt may form a part of the Bastar Craton and does not represent exhumed oceanic crust of the Bundelkhand Craton. It is further shown that rocks of the BBG belt have undergone an earlier high-grade granulite metamorphism at 2672 ± 54 Ma (Sm-Nd age) and a post-peak granulite metamorphism at 1416 ± 59 Ma (Sm-Nd age, 1380 ± 28 Ma Rb-Sr age). These events were followed by deposition of the Sausar supracrustals and Neoproterozoic Sausar orogeny between 973 ± 63 Ma and 800 ± 16 Ma (Rb-Sr ages).

1. Introduction

Precambrian crustal evolution is characterized by successive development of supracrustal belts and orogens often associated with development of high-grade metamorphic belts. Regional and global correlation of such events is an onerous task as younger tectono-metamorphic events often overprint (and rotate) earlier structures and result in degradation of earlier mineral assemblages (Harley 1992; Harley and Fitzsimons 1995). Study of all components of complex Precambrian tectono-metamorphic belts is thus essential for building coherent regional scale models. Recent work in the Sausar Mobile Belt (SMB) in central India (Bhowmik *et al* 1999, Roy *et al* 2000), has shown that granulite belts in the northern and southern parts of the SMB respectively, retain peak metamorphic imprints of pre-Sausar orogeny and that there is a distinct gap in metamorphic grade between the granulite belts and the Sausar Group of rocks. These studies have thus inferred that the

Keywords. Granulite; Sausar, Bhandara; Balaghat; tholeiite; migmatite; orogeny.

Proc. Indian Acad. Sci. (Earth Planet. Sci.), **110**, No. 4, December 2001, pp. 351–368

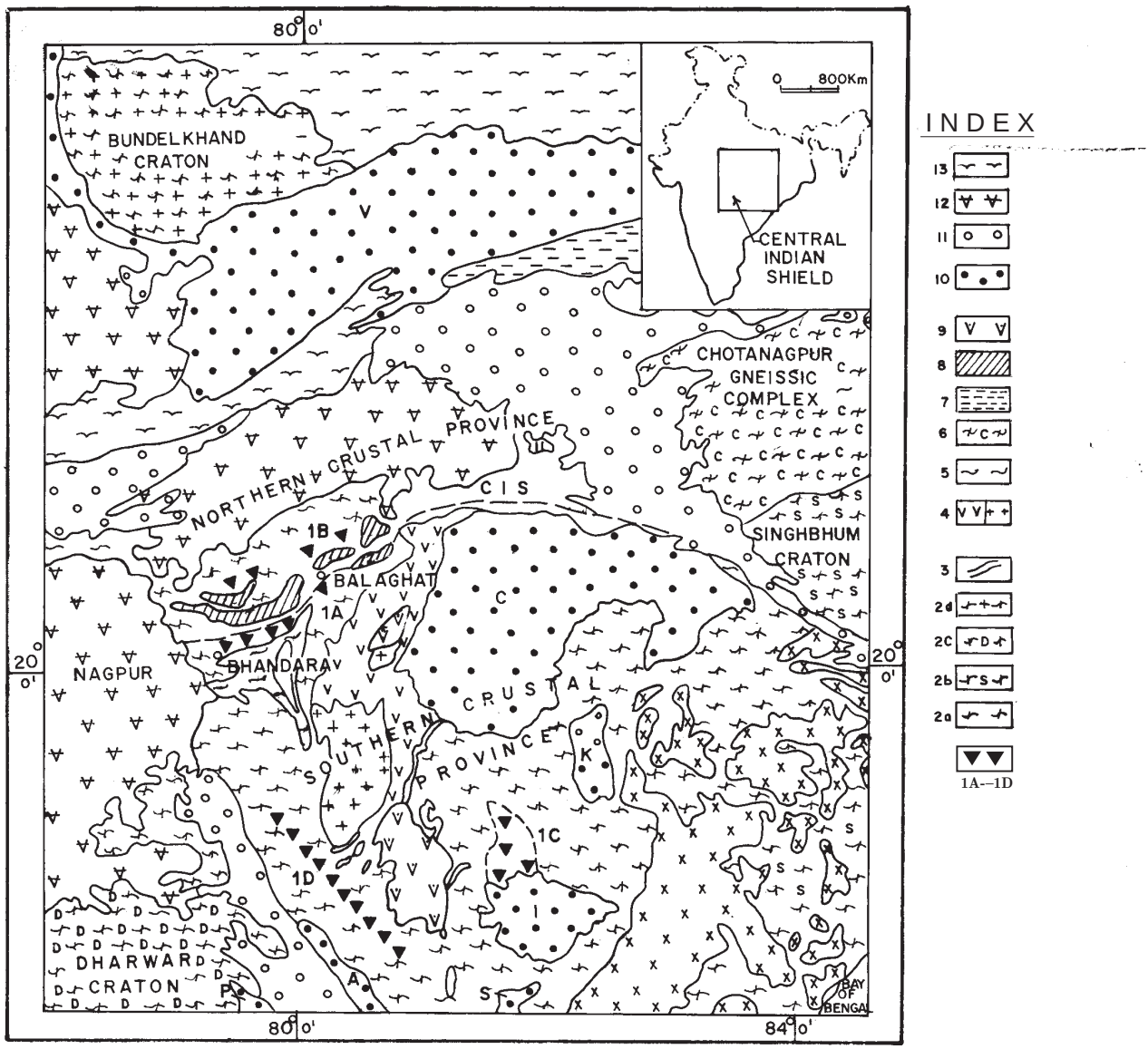

Figure 1. Geological map of central India showing cratonal and major lithotectonic components. **(1)** Granulite Belt (A) Bhandara-Balaghat Belt, (B) Ramakona-Katangi Belt, (C) Kondagaon Belt (D) Bhopalpatnam Belt. **(2)** (a) Sukma-Bengpal Group (Bastar Craton), (b) Singhbhum Craton, (c) Dharwar Craton. (d) Bundelkhand Craton **(3)** Bailadila Group. **(4)** Dongargarh Super Group. **(5)** Sakoli Group. **(6)** Chhota Nagpur Gneissic Complex. **(7)** Mahakoshal Group. **(8)** Sausar Group. **(9)** Abujhmar, Kairagarh. **(10)** Vindhyan (V), Chhatisgarh,Indravati(I), Sabari (S), Khariar (K), Albaka (A), Pakhal (P). **(11)** Gondwana. **(12)** Deccan Trap. **(13)** Alluvium.

evolution of the SMB was polycyclic in nature. This paper presents an account of the southern marginal granulite belt of the SMB represented by the Bhandara-Balaghat granulite (BBG) belt and discusses the role of this granulite belt in the evolution of the SMB and the adjoining Bastar craton.

2. Geological setting

The Precambrian crust in central India is represented by the northern Bundelkhand and the southern Bastar Craton, separated by the SMB (Roy *et al* 2000). The Bastar craton comprises Palaeo- to Mesoarchaean Sukma gneiss-granitoids and supracrustals, Bhopalpatnam and Kondagaon granulite belts, the Bailadila Group of Iron formations, the Chandenar-Tulsidongar mobile belt (including the Bengpal Group), younger supracrustals of the Dongargarh and Kotri Supergroups (including the Dongargarh and Malanjkhand granitoids), and cover sediments (Mishra *et al* 1988; Prakash Narasimha *et al* 1996; Ramachandra *et al* 1998) (figure 1). The margins of the Bastar craton show involvement in the Eastern Ghat mobile belt orogeny in the east and

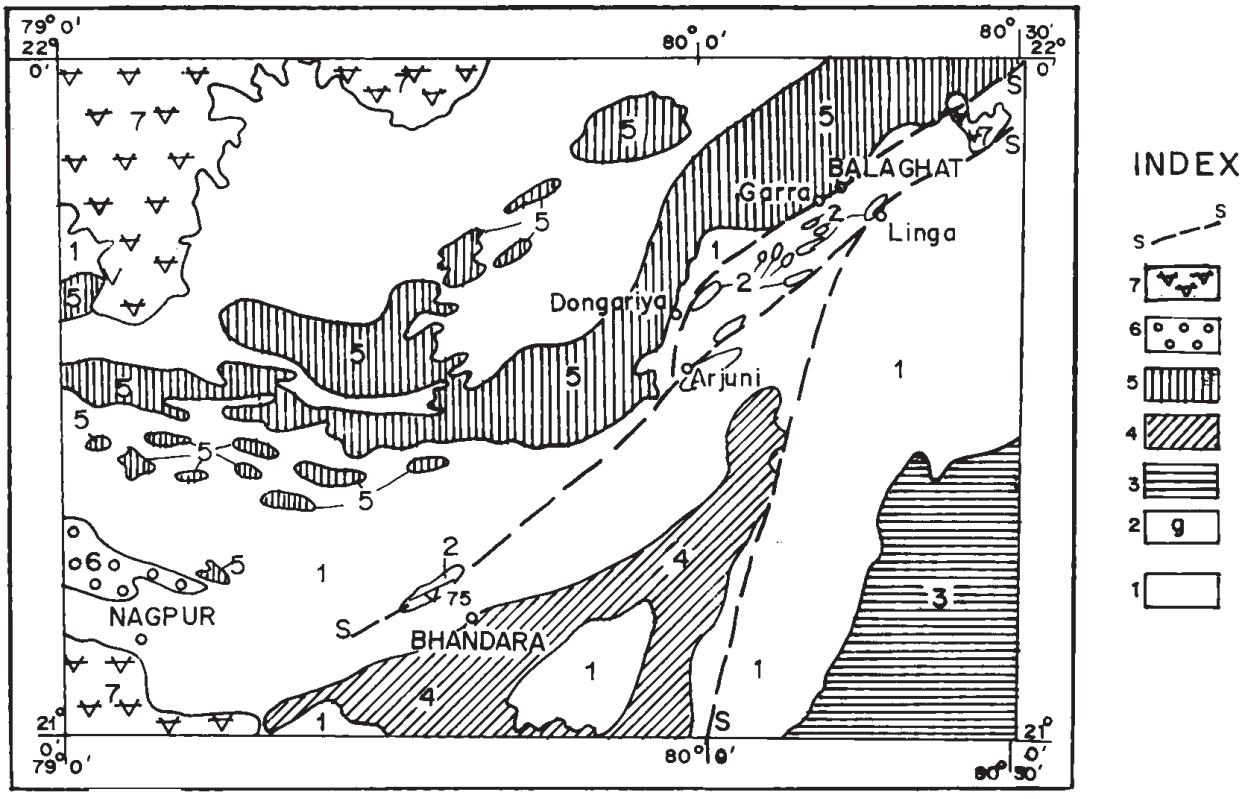

Figure 2. Geological map of central India showing disposition of the Bhandara- Balaghat granulite (BBG) belt. **(1)** Migmatite-Granite Gneiss (Tirodi & Amgaon gneiss). **(2)** Granulite facies rocks of BBG belt. **(3)** Dongargarh Supergroup. **(4)** Sakoli fold belt. **(5)** Sausar belt. **(6)** Gondwana. **(7)** Deccan Trap. **(8)** s-s Major ductile shear zone.

southeast, the Proterozoic and younger orogenies in the southwest and the Sausar mobile belt (SMB) orogeny in the north (Ramachandra *et al* 1998). The Bundelkhand craton (figure 1) comprises Palaeo- to Mesoarchaean Bundelkhand and Sidhi associations, younger supracrustals of the Mahakoshal Group along with intrusive granitoids, cover sequences of Bijawar and Gwalior Groups and Meso- to Neoproterozoic Betul-Chhindwara and Bilaspur-Raigarh-Surguja mobile belts and the Vindhyan cover sediments. The marginal relations of the Bundelkhand craton at its south with the SMB are yet poorly understood, but are characterized by ductile shearing and tectonic interleaving of older and younger components (Roy *et al* 2000).

The SMB separating the Bastar and the Bundelkhand cratons occurs as a curvilinear, ENE–WSW to E–W trending, almost 300 km long and 70 km wide belt, and is comprised of three main components, including the northern Ramkona granulite belt, central Sausar Group of supracrustals and southern Bhandara-Balaghat granulite (BBG) belt (Bhowmik *et al* 1999; Roy *et al* 2000) (figure 2). The Sausar Group of rocks, forming the central part of the SMB is represented by an older metamorphic group including the Tirodi gneiss-migmatites and supracrustals, and a sequence of intensely deformed younger platformal facies supracrustals intruded by granitic rocks (Narayanaswamy *et al* 1963). Huin *et al* (1998), Khan *et al* (1998, 1999), and Bhowmik *et al* (1999) have recorded three generations of structure from the Sausar Group showing successive overprinting relations and have established that the first generation structure in the Sausar Group overprints early mylonitic fabric in the Tirodi gneiss-migmatite and northern Ramkona granulites. Four episodes of metamorphism, namely, M1, M2, M3 and M4, have been recorded from the Sausar Group of rocks with peak upper amphibolite facies event during M2. Bhowmik *et al* (1999) have shown that the Ramkona granulites at the northern margin of the SMB comprise a sequence of mafic granulite, and felsic migmatitic gneiss interleaved with the Sausar Group of rocks. They have also shown that the granulites record pre-Sausar structures and metamorphic imprints with the peak M2 event recording ~10.5kb pressure and 775° C temperature. They have further inferred that the granulites formed the basement for deposition of Sausar supracrustals and were tectonically imbricated with the latter during the Sausar orogeny correlated with the 1000 Ma Grenvellian event.

Geochronological data for the SMB is meager and includes the Rb/Sr whole rock isochron age of 1525 ± 70 Ma and mineral isochron age of 860 Ma

by Sarkar *et al* (1986) for the Tirodi gneiss, the former considered to mark the main phase of amphibolite facies metamorphism in the Sausar Group and the latter mineral age as representing the terminal thermal overprint of the Sausar orogeny. Lippolt and Hautmann (1994) have obtained Ar/Ar age of 950 Ma for cryptomelane from the Sitapur mines and interpret the age to represent the closure of Satpura (≡Sausar orogeny) cycle amphibolite facies metamorphism. Recent geochronological data for the BBG belt include Sm-Nd dates of 2672 ± 54 Ma and 1416 ± 59 Ma, and Rb-Sr date of 1380 ± 28 Ma for charnockite and two-pyroxene granulite of the BBG belt, representing different ages of granulite facies metamorphism; and Rb-Sr dates of 800 ± 16 Ma for charnockites and 973 ± 63 Ma for mafic granulites in the northern shear zone of the BBG belt, representing development of amphibolite facies assemblages in granulites (Abhijit Roy, personal comm.).

3. Lithology and field relations

The Bhandara-Balaghat granulite belt, forming the southern margin of the SMB, extends discontinuously for more than 100 km from northwest of Bhandara in the southwest, in Maharashtra, to east of Balaghat in the northeast, in Madhya Pradesh. It was earlier included as a part of the older metamorphics at the base of the Sausar Group (Narayanaswamy and Venkatesh 1971). Rajurkar (1974) and Mohabey and Dekate (1984) recorded the presence of two-pyroxene granulite near Bhandara. Jain *et al* (1995) showed that granulite rocks of this belt occur as lensoid bodies within gneisses extending discontinuously from Bhandara in the southwest to Ratanpur in the northeast. They also reported the presence of two-pyroxene granulites, orthopyroxene and garnet bearing BIF, cordierite bearing metapelites and gneisses and have inferred that the granulites represent oceanic basalt, now occurring, along with associated metasediments, as exhumed blocks within migmatites. Yedekar and Jain (1995) have interpreted Ar/Ar age of 1300 Ma obtained from hornblende in two-pyroxene granulite as representing the episode of post-granulite retrogressive event.

The Bhandara part of the BBG is represented by a large two-pyroxene granulite body elongate along ENE–WSW, extending along strike for about 5 km, with a maximum width of 1.5 km, exposed near Bhandara and is locally associated with migmatitic gneisses and a thin band of quartzite. The two-pyroxene granulite is medium to coarse grained and shows uniform gabbroic composition with occasional relict ophitic and sub-ophitic texture. Small (a few cm thick) gabbro-anorthositic gabbro layers together with rare segregations of pyroxene up to 10 cm in size occur at places. The main foliation trends from NE–SW to N70°E–S70°W with steep southerly dips and plagioclase and pyroxenes show protomylonitic character along local sinistral shears sub-parallel to the main foliation, as evidenced by recovery and recrystallization and bending of twin lamellae in plagioclase. The two-pyroxene granulite shows a mineral assemblage of Pl-Opx-Cpx-Hbl-Opq ±Scp±Grt.

The granite gneiss in the northern margin of the BBG belt is in tectonic contact with mylonitised low-grade metasediments of the Sausar Group showing development of protomylonitic fabric in both metasediments and granite gneiss and a low-northerly plunging stretching lineation. The granite gneiss delimiting the southern margin of the BBG belt also shows mylonitic and phyllonitic character. The full spectrum of rocks of the BBG belt is best exposed in the Arjuni-Balaghat area (figure 2) and comprises a sequence of quartzite, BIF, metapelite, two-pyroxene granulite, charnockite and charnockitic gneiss and migmatitic and granitic gneiss. These are shown in table 1 along with their main mineral assemblages.

The different rock types mentioned above occur interbanded mainly within migmatitic and granite gneisses. Granite gneiss is mainly exposed in the northern part and southern margins of the BBG belt are strongly tectonised on ENE–WSW trending planes. The migmatitic gneiss includes impersistent salic-mafic bands a few mm to a few cm thick. The pegmatitic salic bands contain up to 10 cm long deformed K-feldspar phenocrysts. Melt formation is indicated by the presence of nebulous and fleck structures in the rocks, biotite grains around K-feldspar phenocrysts and melt supported texture (e.g. tabular feldspars, granitic intergrowth texture) in the quartzofeldspathic salic bands.

Quartzite is rare and occurs as bands up to 10 m in size as near Bhandi. BIF is exposed as a major folded band extending for a few 100 m near Larsara and as small bands near Amgaon. The rock is coarse grained and contains orthopyroxene and garnet grains measuring up to 5 cm in size, along with smaller grains of quartz, hornblende and cummingtonite-grunerite. Metapelites are associated with granitic leucosomes and commonly occur as interbands less than a metre long with gneisses and other granulites. They are best exposed in the Hurkitola, Dongargaon, Larsara and Mendki areas. Al-metapelites are medium grained and schistose with sillimanite, kyanite and micas measuring from a few mm to 0.5 cm in size. Cordierite bearing rocks are finer grained and less schistose. Two-pyroxene granulites occur as long, linear bands, several hundred metres in length mainly in the central part of the BBG belt, near Lingmara, Mendki, Larsara and Dongariya. The rocks show relict ophitic and sub-

Table 1. *Generalized tectonically significant lithosuccession and mineral assemblage in rocks of the BBG belt.*

Lithology	Mineral assemblage
Charnockite and charnockitic gneiss (intrusives of acid and intermediate composition)	Qz-Pl-Kfs-Pth-Opx-Cpx-Grt-Hbl-Bt-Opq-Apa- Zir-Sph
Two-pyroxene granulite (metabasics)	Qz-Pl-Opx-Cpx-Gar-Hbl-Opq-Apa-Bt
Mg-Al and Mg-metapelites	Qz-Crd-Anth/Cum/Grun-Bt-Chl-Opq-Apa Qz-Pl-Kfs/Pth-Crd-Opx-Grt-Spl-Gph-Sil-Bt-Mus-Rt-Opq
Al-metapelites	Qz-Sil-Ky-Kfs-Pl-Bt-Mus-Crn-Grt-Rt-Opq-Apa-Zir
Banded iron formation	Qz-Opx-Grt-Hbl-Cum/Grun-Mag
Quartzite	Qz±Fuch±Chl±Grt
Migmatite and granite gneiss	Qz-Kfs/Pth-Pl-Grt-Bt-Hbl-Apa-Sph- Zir

ophitic texture, variably developed foliation and local layering due to metamorphic differentiation. Charnockite and charnockitic gneisses are medium grained rocks of intermediate to acidic composition and have the typical greasy charnockitic appearance. They are weakly or strongly foliated and are typically interbanded with two-pyroxene granulite and migmatitic gneiss in Arjuni, Dongariya and Larsara areas, and also occur as small patches or stocks.

4. Structural set up

The BBG belt is located in the Central Indian Shear Zone (CIS) that is marked by the development of mylonites and comprises multiple shear zones having polycyclic histories. The present study has shown that there are at least two prominent ENE–WSW trending ductile shear zones within the Central Indian Shear Zone. The first one marks the boundary between the Sausar belt in the north and basement gneisses with granulites in the south. The second one delineates the boundary between granulite belt in the north and the Amgaon Gneissic Complex (AGC) in the south. Thus, there are two prominent ductile shear zones, which border the granulite belt, one in the north and other in the south. The northern shear zone has steep northerly dip, though at places, reversal in the attitude has been noted. The stretching lineation on this steeply dipping mylonite plane is invariably steep. The lineation data, in conjunction with shear bands suggest predominant dip-slip component with northern Sausar belt going down with reference to the granulite belt. In contrast, the steep northerly dipping shear zone on the south of the granulite belt exhibits a reverse sense of movement, wherein the granulite belt has been thrust over the Amgaon gneisses. Based on the difference in the kinematics it is interpreted that these shear zones were developed at different times and sequentially accreted different tectono-metamorphic terrains together.

The granulites exhibit a prominent ENE–WSW striking sub-vertical foliation/layering defined mainly by amphiboles. This layering shows mylonitic structure including S-C fabric in different rocks. At least one set of small folds is developed on this foliation plane. These folds have E–W to ENE–WSW striking sub vertical axial planes and moderate to steep (even vertical) plunge of the fold axes. Thin section study has shown that the amphiboles defining the above layering post-date granulite assemblages. Further, mesoscopic structures related to granulite facies metamorphism could not be recognised. This indicates that the amphibolite grade structures post-date those of the granulite facies metamorphism.

5. Petrography

The two-pyroxene granulite and the charnockitic rocks show superposition of deformation fabric over igneous melt supported textures, which are locally preserved in the form of ophitic, subophitic and intergrowth textures. Metamorphic fabrics include granoblastic texture, mineral reactions involving neocrystal growth of coronitic or porpyroblastic minerals, exsolution texture and development of perthite and myrmekites. Protomylonitic texture is common along shear zones and is represented by incipient recovery and recrystallization in quartz and feldspars, development of kink bands and asymmetric tails in pyroxene, mica and hornblende.

Metapelites show granoblastic texture and development of sillimanite, kyanite, cordierite and garnet porphyroblasts in rocks of appropriate

(Al- or Al-Mg) compositions. Reaction textures involving coronitic or symplectitic growth involving orthopyroxene, sillimanite, cordierite, garnet, sphene, rutile and opaque are well preserved. Presence of pegmatite, rare aplite and small bands and pools of granitic leucosomes (neosomes) up to a few cm in dimension showing melt supported fabric indicate generation of partial melts. Mylonitic fabric including development of S-C fabric, 'fish' structure, kink bands etc. in orthopyroxene and mica is also present.

6. Geochemistry

Twenty nine major and trace analyses of pyroxene granulites, charnockites and granitoids from the BBG belt are presented mainly to study if magmatic or tectono-magmatic relationships exist between different lithocomponents. The analyses were carried out at the chemical laboratories of the GSI, Central Region, Nagpur, by XRF methods using suitable internal standards. Of the 29 samples, 15 represent different types of granitoids including migmatitic leucosomes and granite gneisses; 10 of two-pyroxene granulites including 6 from Arjuni-Balaghat area and 4 from Bhandara; and 4 of charnockite and charnockite gneiss. The analytical results are given in table 2 and CIPW Norms in table 3.

The granitoids show a range in SiO_2 composition varying from 63.53% to 74.08% with Al_2O_3 ranging from slightly above 11% to 16.98%. These rocks are typically low in iron and magnesium and are generally low in calcium. K_2O is commonly higher than Na_2O and total alkalis range from slightly above 4.5% to 8.5%. Sr content (varying from 130 ppm to 620 ppm) is usually higher than that of Rb (60 ppm to 490 ppm) and Zr varies from 10 ppm to 420 ppm. Cr shows a variation from 10 ppm to 240 ppm. The two-pyroxene granulites show a silica range between 47.60% and 53.64% with MgO varying from 7.03% to 12%. They are moderately iron rich and show low- to moderate TiO_2 and typically low alkalis. The values of Mg # ranging from 48 to 69 for these rocks indicates their evolved nature. Sr content is commonly higher than that of Rb in the two-pyroxene granulites and Cr values range from 20 ppm to 960 ppm. Zr varies from 30 ppm to 280 ppm. The SiO_2 in the charnockites ranges from 63% to 74.15% with a narrow spread in Al_2O_3 content. MgO is low with variable low- to high contents of Iron oxides and calcium. K_2O tends to be higher than Na_2O and total alkali contents are generally similar. Sr and Rb contents are generally similar in the charnockites with Cr varying from 20 ppm to 80 ppm. Zr shows a variation from 60 ppm to 230 ppm.

The plots of analyses of all the above rocks in the SiO_2 vs. total alkali diagram after Wilson (1989), as given in figure 3 distinctly occur in two separate clusters, in the gabbro and granite compositional fields. The two-pyroxene granulites occur in a relatively tightly clustered group in the gabbro field whereas the granitoids and the charnockites occur in the granitic field, showing a restricted compositional spread in the acidic range from quartz-diorite (granodiorite) to granite. Thus a bimodal relationship between the basic and acidic compositions is indicated. In the AFM diagram after Irvine and Baragar (1971) (figure 4) the basic and acidic compositions clearly follow different trends and further depict the bimodal relationship between the two. The basic trend is typically tholeiitic, shows an evolved nature and lacks Fe enrichment commonly observed in differentiated high-level mafic complexes. Normative CIPW values indicate qz-normative and hence saturated nature of the two-pyroxene granulites. The charnockites and granitoids show a mixed tholeiitic and calc-alkaline nature, but as the granitoid sample includes a variety of sources ranging from leucosome of para- or ortho-migmatites and granite intrusives, the trends at best can be taken as suggestive.

The two-pyroxene granulites in Jensen's (as modified by Jensen and Pyke 1982) diagram (figure 5) generally show tholeiitic character excepting two plots that occur in the komatiite field. But as these two rocks are characterized by relict ophitic and subophitic textures typical of tholeiites and lack spinifex or related textures they are inferred to be of tholeiitic affinity only. A majority of the other samples show high-Mg rather than high-Fe tholeiitic character. Most of the two-pyroxene granulites plot in the continental basalt field of TiO_2-P_2O_5-K_2O diagram (figure 6) after Pearce *et al* (1975), indicating the continental-tholeiite character of these rocks. The restricted compositional spread among acidic compositions is brought out in the Ab-An-Or diagram after Barker (1979) (figure 7). The paucity of tonalite and trondhjemite possibly indicate thorough crustal reworking of protoliths for the acidic rocks and likely influence of continental processes in generation of precursor magma for charnockite rocks. CIPW norm calculations indicate that most of the acidic rocks including charnockites are corundum normative. They mainly occur in the peraluminous field of SiO_2 vs. *A/CNK* diagram (figure 8) and a larger number show *S*- rather than *I*- type character (after Chappel and White 1974). These mixed signatures and especially the high Al nature of the rocks compared to their alkali content reflects the variable para- and ortho- nature of the samples. The plots of granitic and charnockite compositions in the Q-Ab-Or diagram (figure 9) after Anderson

Table 2. *Major and trace element analyses of two-pyroxene granulites and charnockites from the BBG belt.*

Sample	**TP-1**	**TP-2**	**TP-3**	**TP-4**	**TP-5**	**TP-6**	**TP-7**	**TP-8**	**TP-9**	**TP-10**	**CH-1**	**CH-2**	**CH-3**	**CH-4**	
SiO_2	47.60	47.85	48.03	48.36	49.08	49.82	50.00	50.75	50.86	53.64	63.00	63.09	72.14	74.15	
Al_2O_3	16.30	14.97	11.42	14.49	13.50	13.85	12.78	12.09	12.39	14.25	14.00	16.07	13.65	13.19	
FeO	9.90	9.00	8.82	12.6	6.02	9.90	5.22	10.08	7.92	6.30	6.12	4.32	1.98	1.98	
Fe_2O_3	2.64	3.31	3.34	2.62	4.67	4.84	4.41	4.80	6.01	3.09	2.39	2.88	0.82	0.66	
TiO_2	0.85	1.16	1.87	1.79	0.97	1.36	0.11	1.34	1.25	1.36	1.10	1.18	0.28	0.28	
CaO	12.08	11.87	12.30	8.90	14.05	10.20	16.50	10.56	6.40	7.50	5.80	5.10	2.46	1.71	
MgO	8.38	9.36	11.50	7.26	8.04	7.2	8.32	7.03	12.00	9.10	2.41	1.89	0.65	0.65	
K_2O	0.07	0.07	0.11	0.12	0.14	0.14	0.01	0.67	0.44	1.39	2.31	2.47	3.85	3.73	
Na_2O	1.43	1.28	0.85	1.82	1.91	1.75	1.15	2.17	1.09	0.50	2.51	2.67	2.83	2.90	
MnO	0.16	0.16	0.36	0.13	0.21	0.13	0.92	0.14	0.15	0.11	0.09	0.06	0.01	0.01	
P_2O_5	0.25	0.20	0.42	0.29	0.25	0.29	0.20	0.15	0.41	0.84	0.25	0.20	0.20	0.15	
$+H_2O$	0.30	0.22	0.34	0.33	0.85	0.33	0.33	0.01	0.43	0.31	0.22	0.34	0.30	0.32	
Total	99.96	99.45	99.36	98.71	99.69	99.81	99.95	99.78	99.35	98.39	100.20	100.27	99.17	99.73	
Mg#	57.00	61.00	67.00	48.00	64.00	52.00	67.00	51.00	67.00	68.00	-	-	-	-	
Nb	—	—	—	—	—	—	—	20	—	40	30	40	10	10	
Sr	80	120	20	110	40	90	20	240	210	710	280	280	210	180	
Rb	20	10	20	10	130	20	120	70	20	80	270	290	160	150	
Cr	320	400	80	250	20	200	20	210	960	860	70	80	30	20	
Zr	40	40	60	60	170	60	180	30	60	280	80	60	230	140	
Y	20	10	30	20	10	20	10	70	10	—	30	20	30	40	
Sample	**G-1**	**G-2**	**G-3**	**G-4**	**G-5**	**G-6**	**G-7**	**G-8**	**G-9**	**G-10**	**G-11**	**G-12**	**G-13**	**G-14**	**G-15**
SiO_2	63.53	65.99	66.57	66.98	74.64	68.83	68.99	70.00	70.83	71.26	71.77	72.46	72.94	73.27	74.08
Al_2O_3	16.98	14.05	14.92	14.20	11.29	13.86	13.69	14.38	13.55	13.81	14.48	12.93	12.89	14.61	13.35
FeO	3.06	5.58	2.52	4.14	1.44	3.42	3.06	3.24	1.98	2.16	0.36	3.42	0.90	0.54	1.44
Fe_2O_3	2.29	1.73	2.83	2.36	0.87	0.33	0.63	1.03	0.81	1.05	2.52	1.47	0.94	1.05	2.73
TiO_2	1.29	1.45	0.95	0.70	0.24	0.62	0.84	0.55	0.67	0.77	0.27	0.23	0.32	0.29	0.01
CaO	4.34	3.82	2.64	2.37	2.50	4.60	2.80	1.57	1.70	2.20	1.50	1.84	2.00	1.36	1.00
MgO	2.10	1.81	1.67	2.34	0.61	0.88	0.73	1.02	0.54	0.51	0.66	0.43	0.38	0.47	0.35
K_2O	2.51	1.54	4.27	3.31	6.33	4.70	5.85	4.60	6.53	4.32	3.73	3.12	5.49	2.95	4.11
Na_2O	2.04	2.97	2.06	1.76	1.82	2.32	2.18	2.46	1.93	2.56	3.40	2.58	1.70	4.16	2.76
MnO	0.07	0.05	0.06	0.10	0.01	0.04	0.04	0.01	0.01	0.04	0.01	0.05	0.01	0.01	0.01
P_2O_5	0.60	0.35	0.46	0.15	0.09	0.30	0.25	0.25	0.20	0.15	0.20	0.14	0.34	0.10	0.07
$+H_2O$	0.40	0.34	0.32	0.29	0.44	0.29	0.39	0.38	0.62	0.33	0.45	0.50	1.33	0.40	0.28
Total	99.21	99.68	99.27	98.70	100.28	100.19	99.45	99.49	99.37	99.16	99.35	99.17	99.24	99.21	100.19
Nb	40	30	40	20	20	40	30	20	20	30	10	120	10	20	20
Sr	140	260	440	350	340	600	570	190	390	310	270	620	310	430	130
Rb	280	60	490	210	110	190	120	150	120	160	130	140	120	80	220
Cr	120	60	170	140	170	160	240	20	230	160	10	150	10	10	10
Zr	50	420	50	100	10	20	10	310	10	20	300	10	190	180	150
Y	30	10	10	30	50	30	60	50	40	140	30	220	20	—	70

TP = Two-pyroxene granulite; **CH** = Charnockite & charnockitic gneiss; **G-1** = Gar-plag gneiss; **G-2** = Hbl-gneiss; **G-3 & 4** = Gar-gneiss; **G-5 & 8** = Leucosome from stromatic migmatite; **G-6** = Coarse grained leucosomes from stromatic migmatite; **G-7** = Fine grained granite dyke in stromatic migmatite; **G-9** = K- feldspar rich granite; **G-10** = Leucocratic part in migmatitic gneiss; **G-11 &13** = Leucosome in banded gneiss; **G-12** = Coarse leucocratic augen gneiss; **G-14 & 15** = Leuco-granite gneiss.

Table 3. *CIPW norms for two-pyroxene granulites and charnockites of the BBG belt.*

	Sample	**TP-1**	**TP-2**	**TP-3**	**TP-4**	**TP-5**	**TP-6**	**TP-7**	**TP-8**	**TP-9**	**TP-10**	**CH-1**	**CH-2**	**CH-3**	**CH-4**	
	qz	0	1.4	2.09	2.49	1.87	6.03	3.4	2.41	9.05	15.35	22.65	23.13	34.53	37.65	
	ap	0.67	0.67	1	0.67	0.33	0.68	0.33	0.33	1	2.01	0.67	0.33	0.33	0.33	
	ilm	1.66	2.26	3.47	3.47	1.81	2.56	0.15	2.56	2.41	2.56	2.11	2.26	0.6	0.6	
	mt	3.92	4.85	4.85	3.92	6.93	6.93	6.23	6.93	8.77	4.62	3.46	4.15	1.15	0.92	
	an	37	34.47	27.24	31.41	28.07	29.6	29.71	21.4	27.8	32.25	20.29	24.37	11.3	7.69	
	ab	12.05	12.05	7.33	15.72	16.24	14.67	9.95	18.34	9.43	4.19	20.96	22.53	24.1	24.62	
	or	0.55	0.55	0.55	0.55	1.11	0.82	0.05	3.89	2.78	8.34	13.34	14.45	22.79	22.24	
	cor	0	0	0	0	0	0	0	0	0	0.3	0	0.13	0.74	1.56	
	wo	8.46	9.89	13.1	4.79	17.36	8.08	21.43	12.72	0.58	0	2.7	0	0	0	
Di	en	4.8	5.92	8.72	2.34	12.33	4.59	14.43	7.01	0.41	0	1.19	0	0	0	
	fs	3.27	3.45	3.39	2.36	3.47	3.12	5.33	5.08	0.1	0	1.5	0	0	0	
Hy	en	14.5	14.97	20.07	15.95	7.86	13.42	6.26	10.48	29.68	23.13	4.8	4.7	1.6	1.6	
	fs	9.82	8.72	7.82	16.11	2.21	9.23	2.31	7.59	7.81	7.12	6.02	3.69	2.52	2.65	
Ol	fo	0.86	0	0	0	0	0	0	0	0	0	0	0	0	0	
	fa	0.61	0	0	0	0	0	0	0	0	0	0	0	0	0	
	hm	0	0	0	0	0	0	0	0	0	0	0	0	0	0	
	rut	0	0	0	0	0	0	0	0	0	0	0	0	0	0	
	Sample	**G-1**	**G-2**	**G-3**	**G-4**	**G-5**	**G-6**	**G-7**	**G-8**	**G-9**	**G-10**	**G-11**	**G-12**	**G-13**	**G-14**	**G-15**
	qz	30.81	30.07	30.89	34.05	34.96	26.31	26.31	32.41	29.97	34.28	34.38	39.51	38.95	34.68	39
	ap	1.34	0.67	1	0.33	0.21	0.67	0.67	0.67	0.33	0.33	0.33	0.33	0.82	0.33	0.17
	ilm	2.41	2.71	1.81	1.35	0.45	1.2	1.66	1.05	1.2	1.47	0.45	0.45	0.6	0.6	0.02
	mt	3.46	2.54	4.15	3.46	1.26	0.46	0.92	1.61	1.15	1.61	0.46	2.07	1.38	0.92	3.92
	an	17.98	17.33	10.56	11.01	4.17	13.62	10	5.93	7.69	10.09	6.67	8.24	7.73	6.11	4.54
	ab	17.29	25.15	17.81	15.19	15.19	79.38	18.86	20.96	16.24	22	28.82	22	14.67	35.63	23.58
	or	15.01	8.89	25.57	20.01	37.25	27.8	35.02	27.24	38.92	25.57	22.24	18.9	32.8	17.79	24.46
	cor	4.41	1.29	3.05	3.7	0	0	0	3.22	0.54	1.25	2.4	2.27	14.15	2.37	25.66
	wo	0	0	0	0	3.14	3.05	0.85	0	0	0	0	0	0	0	0
Di	en	0	0	0	0	1.5	0.94	0.28	0	0	0	0	0	0	0	0
	fs	0	0	0	0	1.66	2.22	0.59	0	0	0	0	0	0	0	0
Hy	en	5.3	4.5	4.2	5.9	0	1.25	1.51	2.6	1.4	1.3	1.7	1.1	1	1.2	0.9
	fs	1.71	6.6	0.79	4.75	0	2.92	3.23	4.23	2.37	1.88	0	4.88	0.41	0	0.39
Ol	fo	0	0	0	0	0	0	0	0	0	0	0	0	0	0	0
	fa	0	0	0	0	0	0	0	0	0	0	0	0	0	0	0
	hm	0	0	0	0	0	0	0	0	0	0	2.24	0	0	0	0
	rut	0	0	0	0	0	0	0	0	0	0	0	0	0	0.48	0

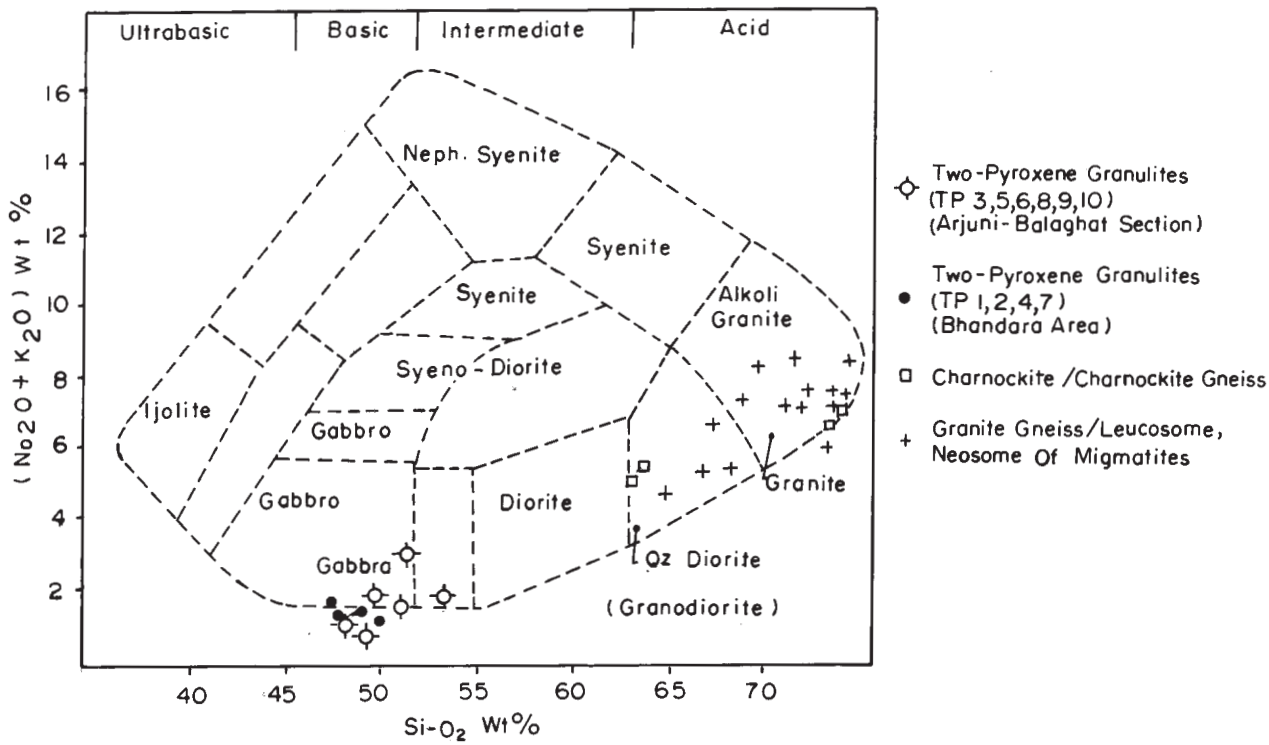

Figure 3. Classification of rocks of BBG belt in SiO_2 vs. total alkali diagram of Cox *et al* (1979) as modified by Wilson (1989). The plots show bimodal character of the basic and acidic compositions of the BBG belt.

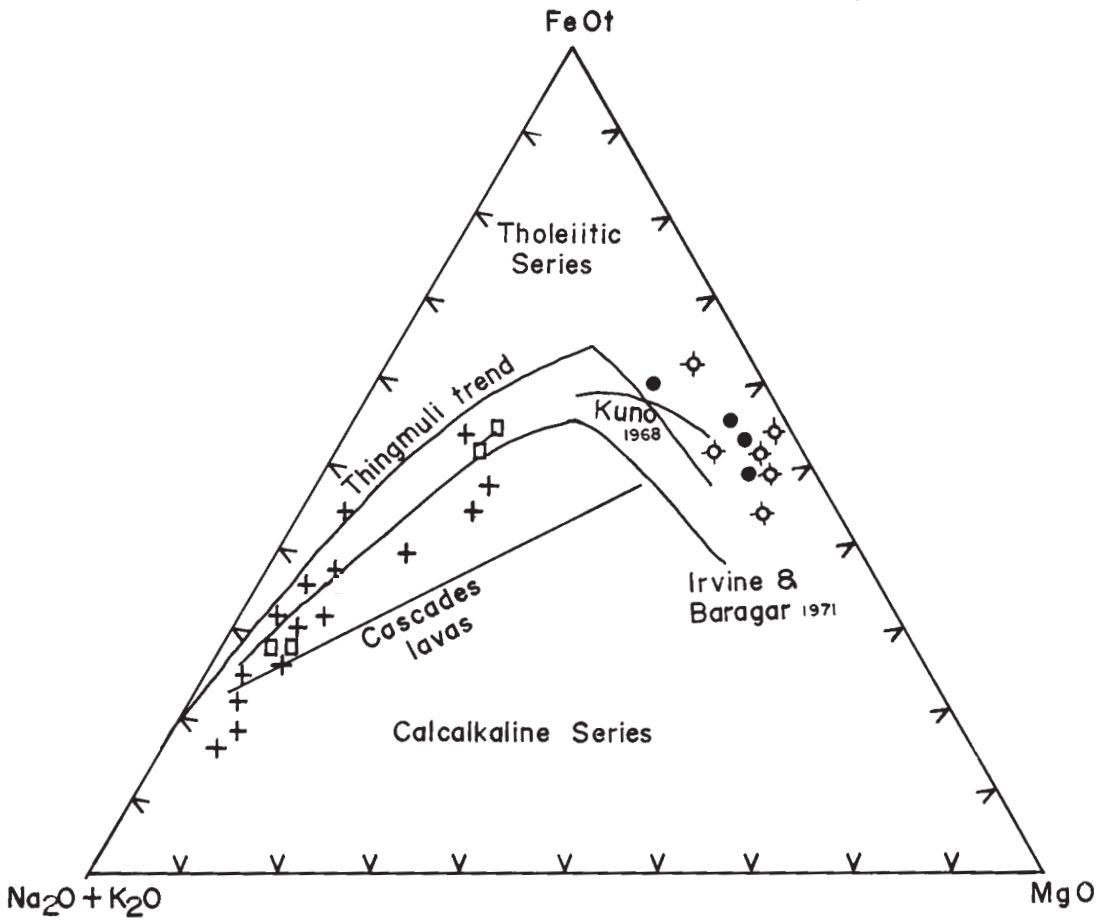

Figure 4. AFM diagram after Irvine and Baragar (1971) showing bimodal relationship between basic and acidic compositions and tholeiitic character of basic rocks of the BBG belt. Symbols as in figure 3.

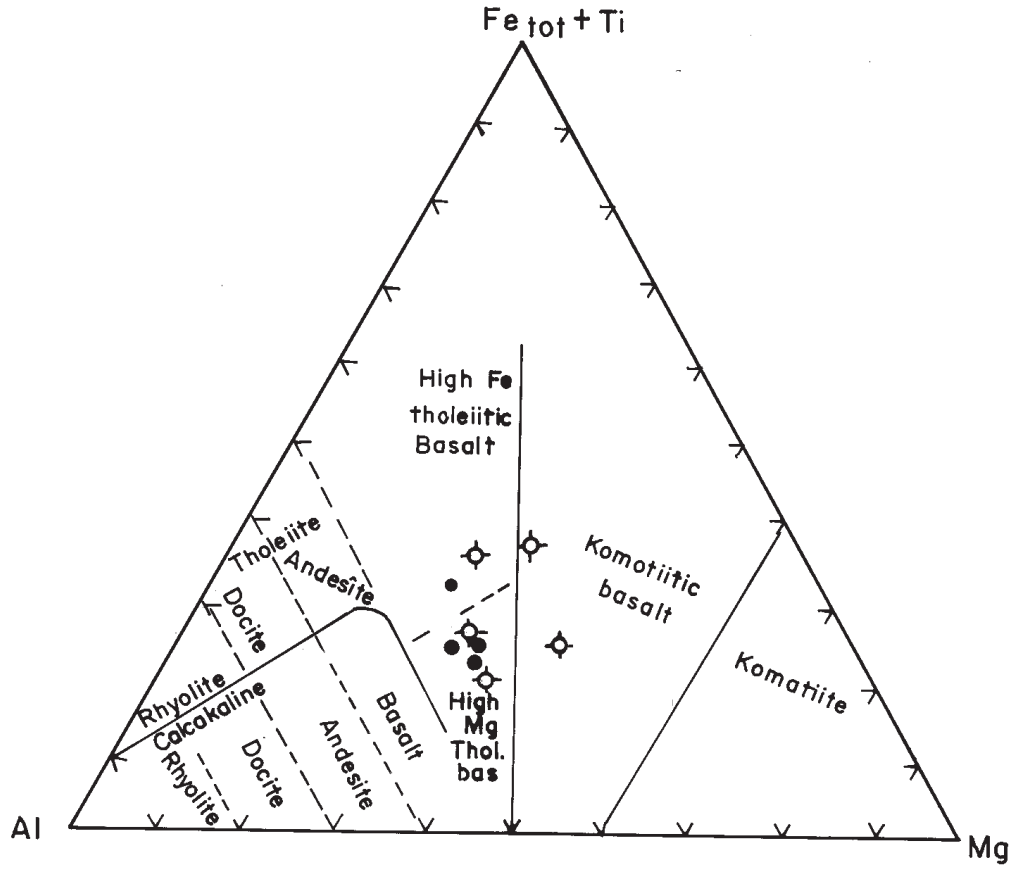

Figure 5. Plots of two-pyroxene granulites and charnockites of the BBG belt in the diagram after Jensen and Pyke (1982) showing predominantly tholeiitic and non-komatiitic nature of the rocks. Symbols as in figure 3.

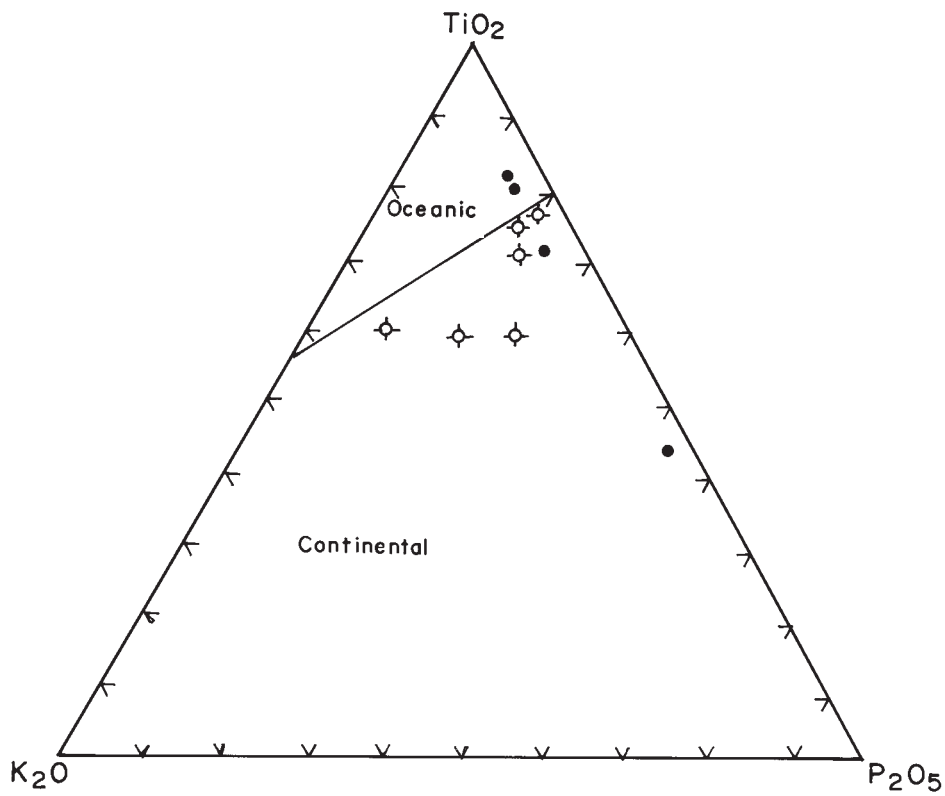

Figure 6. Plots of two-pyroxene granulites and charnockites of the BBG belt in the diagram after Pearce *et al* (1975) show the largely continental setting of the rocks. Symbols as in figure 3.

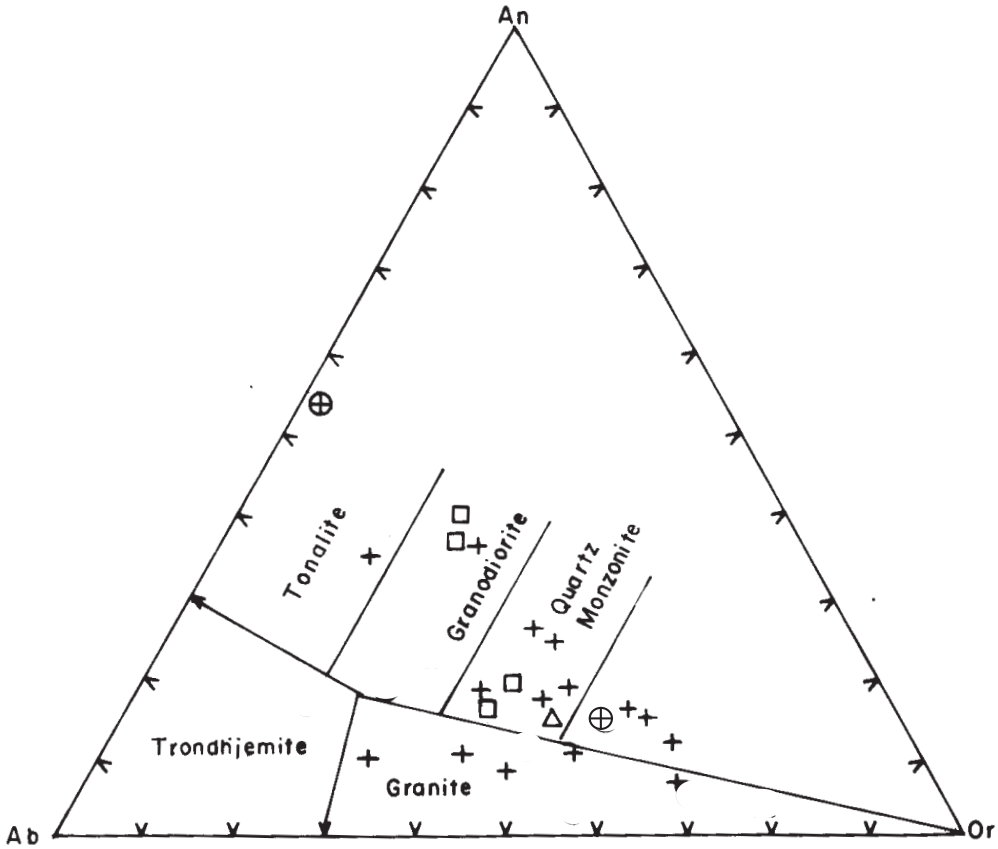

Figure 7. Plots of gneisses and granitoids of the BBG belt in the granite classification diagram after Barker (1979) show restricted compositional spread for these rocks. Symbols as in figure 3.

and Bender (1989), used to determine the depth of magma generation, show some spread. Samples associated with orthomigmatites plot at shallower minima, typically below 2–4 kb minima. The granitoid samples from paramigmatitic association show plots occurring mainly between 4 and 7 kb and 7 and 10 kb minima. However as time of melt generation and movement and effect of fluid during melting are not constrained, further elaboration on this theme is not possible at present.

7. Mineral reactions

Petrographic study of two-pyroxene granulite, charnockite and charnockite gneisses and metapelitic granulites of the BBG belt has resulted in documentation of mineral textures and reactions distinctive of polyphase granulite facies metamorphism in the belt.

Charnockites and charnockitic gneisses contain plagioclase grains showing antiperthitic character. Presence of brown hornblende earlier to porphyroblastic and coronal garnet has been observed in many samples. Hornblende rimmed by orthopyroxene has also been observed (figure 10). This may be due to

$$\text{Ti} - \text{Hbl} + \text{Qz} = \text{Grt} + \text{Opx} + \text{Cpx} + \text{Ilm} + \text{H}_2\text{O} \quad (1)$$

representing a prograde path involving rise in temperature during metamorphism. Interestingly orthopyroxene$_1$, being replaced by orthopyroxene$_2$ has also been observed, and may be related to this event, probably representing the break down of high Al-pyroxene to lower Al-pyroxene.

Mg-Al rich compositions show the presence of porphyroblastic orthopyroxene containing inclusions of cordierite, K-feldspars, perthite, phlogophitic biotite and garnet. This indicates the presence of a pre-existing cordierite-garnet assemblage along with melt. Thus an early reaction as given below was operative:

$$\text{Bt} + \text{Sil} + \text{Qz} = \text{Crd} + \text{Grt} + \text{Kfs} + \text{melt} \quad (2)$$

and may be taken to have heralded the onset of granulite facies metamorphism.

Crd + Grt + Sil + Spl assemblage, without orthopyroxene, is characterized by an early stable

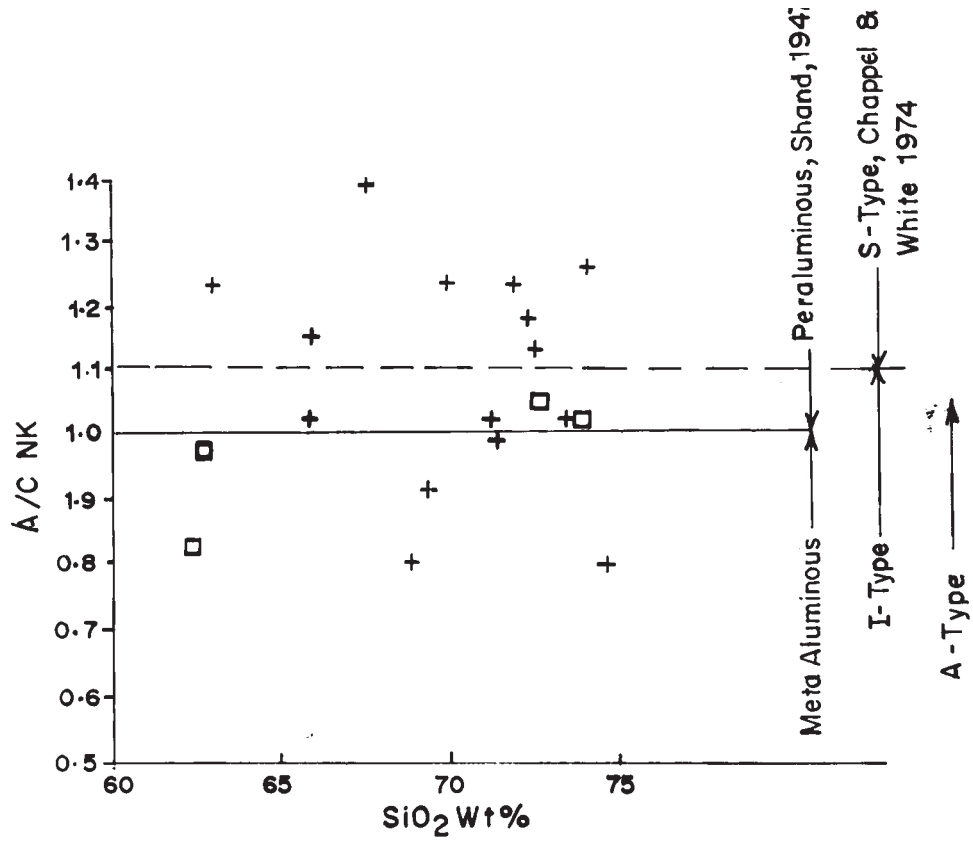

Figure 8. Gneisses and granitoids of the BBG belt in the SiO_2 vs. A/CNK diagram showing mixed, but dominantly peraluminous character of the rocks. Symbols as in figure 3.

assemblage of coarse garnet, sillimanite, cordierite, perthite and opaque association with or without quartz. This assemblage, as in the case of the orthopyroxene bearing one described above, may represent an early melt forming event from reaction (2), given above. Presence of Grt + Crd + Bt bearing quartzofeldspathic (granitic) veins in association with the above metapelites supports this contention.

Orthopyroxene associated with either cordierite or plagioclase (figure 11) in the above set up could have originated through reactions such as,

$$\text{Grt} + \text{Qz} = \text{Opx} + \text{Crd} \quad (3)$$

$$\text{Grt} + \text{Qz} = \text{Opx} + \text{Pl} \quad (4)$$

$$\text{Grt} + \text{Kfs} + \text{v} = \text{Opx} + \text{Crd} + \text{Bt} \quad (5)$$

Alumina rich metapelites show that sillimanite is derived from both inversion of kyanite and from Mus + Qz = Sil + Kfs + melt reaction (cf. Yardley 1989). Garnet either occurs as porphyroblasts or mantles sillimanite and K-feldspar, indicating generation of partial melt by a reaction such as

$$\text{Bt} + \text{Sil} + \text{Qtz} = \text{Grt} + \text{Kfs} + \text{lq} \quad (6)$$

As only kyanite and sillimanite occur as aluminosilicate phases, and as either andalusite or its pseudomorphs have not been identified, it is suggested that aluminous metapelites first passed through the kyanite stability field and with increase in temperature went into the sillimanite field.

Orthopyroxene in different lithologies is rimmed or coronated by second garnet or garnet_2 + quartz + clinopyroxene symplectite. This garnet_2 also shows inclusions of orthopyroxene, cordierite and opaque. The orthopyroxene breakdown may have proceeded by the reaction

$$\text{High Al pyroxene} = \text{low Al pyroxene} + \text{Grt} \quad (7)$$

In the BIF compositions, orthopyroxene shows spectacular deformation lamellae and twins and many grains show stretching along shear planes and 'fish' structure. Garnet occurs as porphyroblasts or as corona around orthopyroxene. Garnet bands replacing kink bands in orthopyroxene also occur. Garnet and orthopyroxene show grain refinement and stability along shear planes. Bluish green hornblende or actinolite-hornblende-Fe amphibole intergrowth replaces orthopyroxene in some samples.

The two pyroxene granulites show reaction textures around orthopyroxene and plagioclase including: fine grained clinopyroxene next to garnet-quartz intergrowths around orthopyroxene (figure 12); clinopyroxene rim around orthopyroxene; and rarely, clinopyroxene-garnet symplectites. In

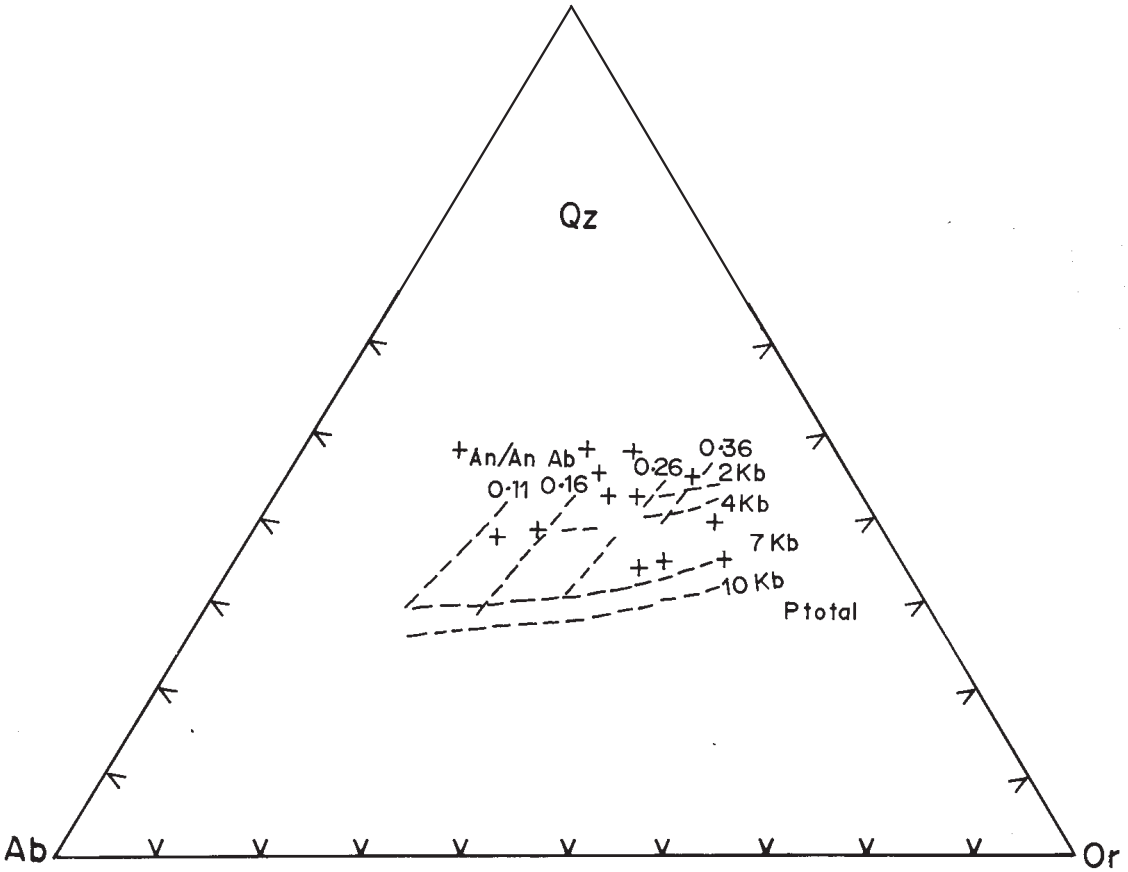

Figure 9. Gneisses and granitoids of the BBG belt in the normative Qz-Ab- Or diagram after Anderson and Bender (1989) showing varied melt generation depths for their protoliths. Symbols as in figure 3.

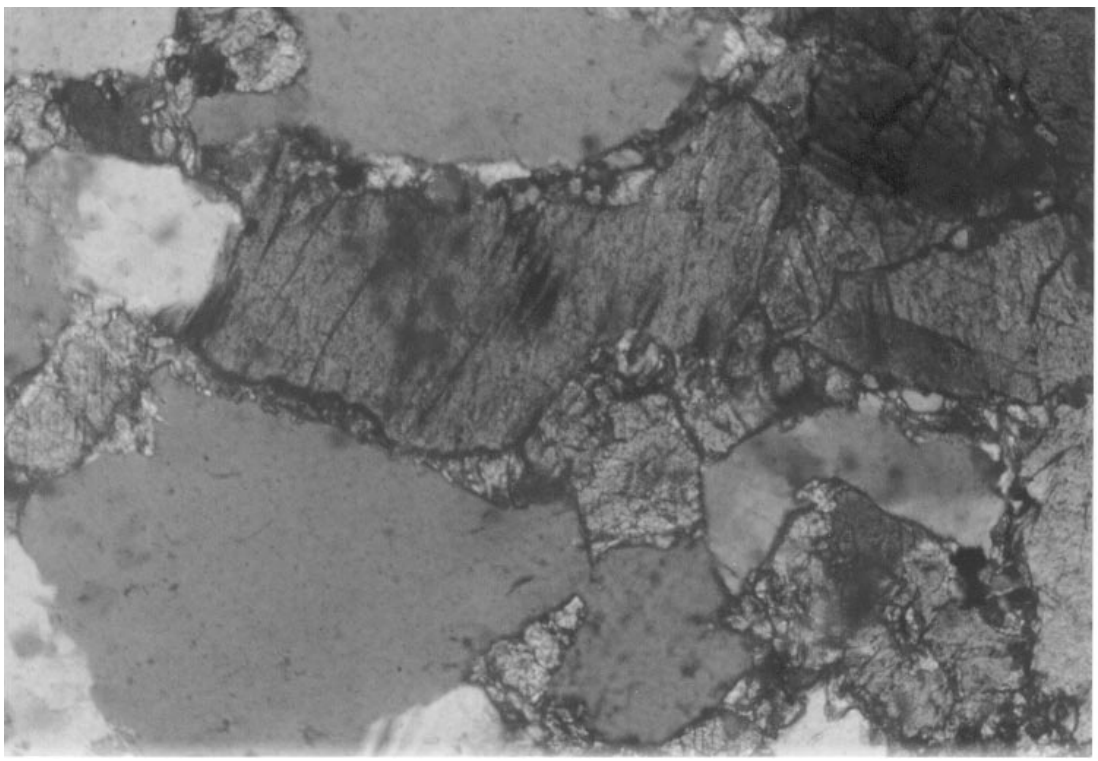

Figure 10. Photomicrograph: Hornblende (large, dark grain slightly above center of the photograph) breaking down to and rimmed by an aggregate of intergrown orthopyroxene, clinopyroxene and ilmenite. Quartz and minor plagioclase occur in other parts of the photograph. [Charnockite, near Larsara, BBG belt.] Width of photograph= 1 mm; semicrossed nicols.

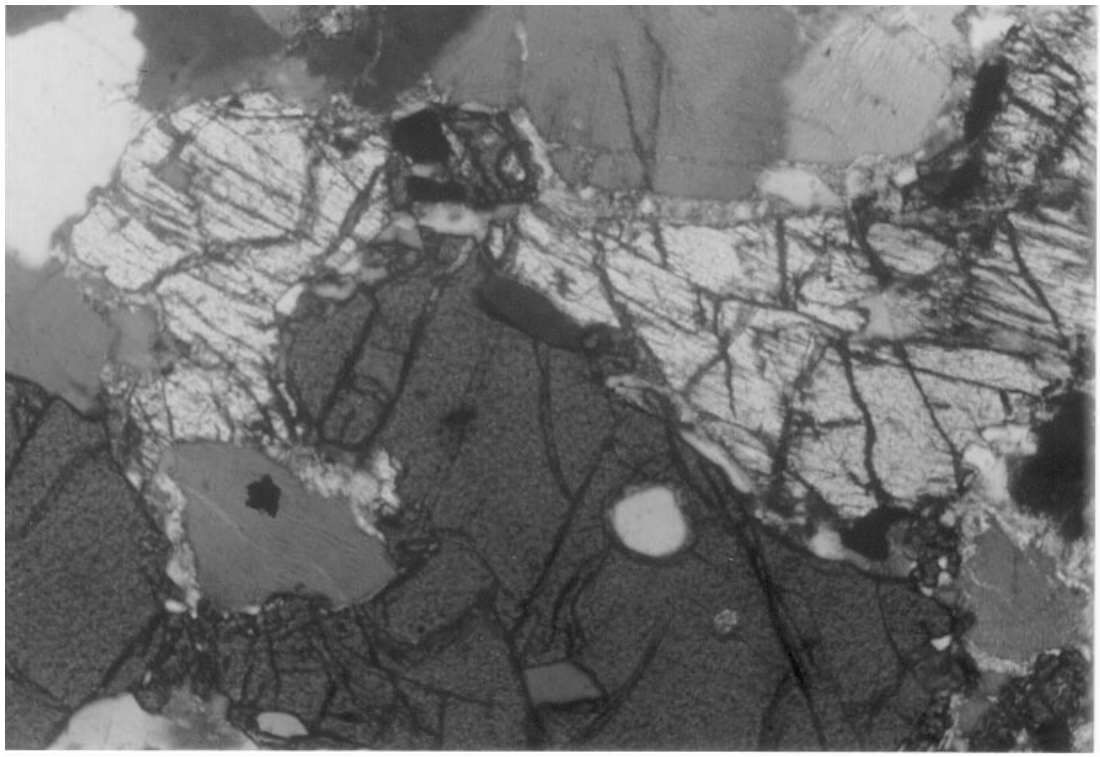

Figure 11. Photomicrograph: Porphyroblastic garnet (dark, platy grain in central and lower parts of the photograph) breaking down to orthopyroxene and plagioclase. [Metapelitic granulite, south of Dongargaon, BBG belt]. Width of photograph=1 mm; semicrossed nicols.

some samples, secondary garnet growth around earlier formed, larger garnet grains is present. Garnet included in some orthopyroxenes may represent garnet formed from re-equilibration of aluminous pyroxene. Presence of hercynitic spinel in orthopyroxene noticed in some samples may also be due to the same reason. Garnet coronas separating orthopyroxene and plagioclase, or, clinopyroxene and plagioclase also occur. These reaction textures are indicative of reactions of the type,

$$\mathrm{Opx} + \mathrm{Pl} = \mathrm{Grt} + \mathrm{Cpx} + \mathrm{Qz} \quad (8)$$

$$\mathrm{Cpx} + \mathrm{Pl} = \mathrm{Grt} + \mathrm{Qz} \quad (9)$$

$$\mathrm{Opx} + \mathrm{Pl} = \mathrm{Grt} + \mathrm{Qz} \quad (10)$$

8. Interpretation of textural data

The reaction textures described from lithological components as discussed from petrographic studies in the above section are all typical of granulite facies (e.g. Harley 1989). All of these also easily plot well within the PT limits considered typical of granulite facies rocks (Bohlen 1987). The high PT equilibrium attained by these rocks is well illustrated by the tholeiitic component of intermediate Mg/Mg+Fe (now two-pyroxene granulite) in the study area, which contain a mineral paragenesis of cpx + gar + qz (Green and Ringwood 1967).

Textural data as documented can further be interpreted as follows:

- The earlier textures indicate breakdown of hornblende to yield garnet, orthopyroxene, clinopyroxene with or without a melt. This is a prograde dehydration reaction involving an amphibolitic protolith. Such a reaction has been documented from the mafic mineral assemblage of banded gneisses.

  A series of reaction textures in Al-rich and Mg-Al rich metapelite involve firstly, melt generation in biotite + sillimanite bearing (amphibolite facies?) protoliths, along with garnet + cordierite assemblage (reaction 6), going on to yield Opx + Crd + Pl assemblages (reactions 7, 8 and 9) with or without melt to complete the prograde path. Kfs/pth + Pl + Crd + Grt bearing granitic leucosomes occurring in close spatial association represent leucosome and melanosomes derived from the above reactions.

  In the next stage, coronitic and symplectitic garnet form over earlier minerals in lithologies of different compositions indicating onset of retrograde (IBC) path. The type charnockite and two-pyroxene granulite in the area show the melt-supported fabric, being directly overprinted by coronitic and symplectitic garnet (reactions 1, 2 and 3). This may indicate that these bodies were emplaced into the above set up at this point of time during the evolution of the granulite belt.

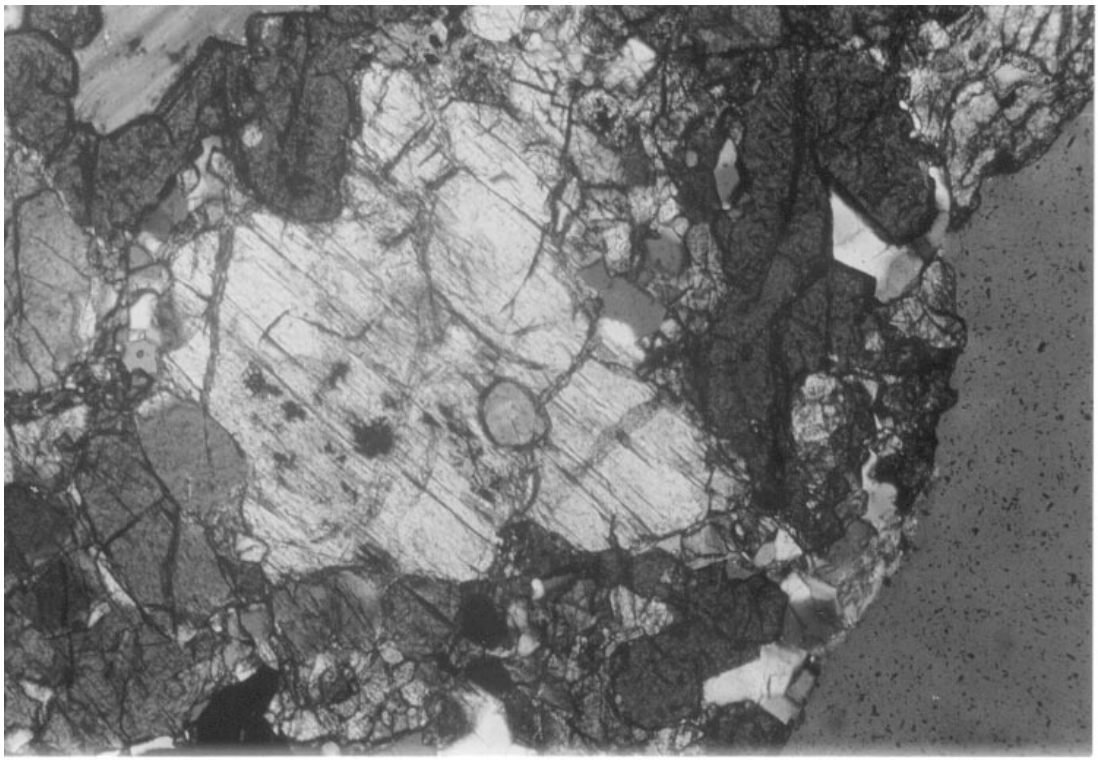

Figure 12. Photomicrograph: Coronotic garnet and clinopyroxene resulting from breakdown of orthopyroxene (center of the photograph)[In two- pyroxene granulite, near Larsara, BBG belt]. Width of photograph= 1 mm; semicrossed nicols.

- Mesoscopic (e.g., in the BIF band) and microscopic evidence in different lithologies show that orthopyroxene, garnet and other high P-T mineralogies as formed above continued to be stable during ductile shearing events.
- Bluish green or brownish green hornblende partially or completely replacing pyroxene; saussuritization and more commonly sericitization of plagioclase; chloritization of garnet; pinitization of cordierite; muscovite alteration of aluminosilicates, are all retrograde events probably connected with juxtaposition of the granulite lithologies with those of the lower grade Sausar supracrustals.

9. Discussion: regional correlation and tectonic evolution of the BBG belt

The BBG belt flanks the southern margin of the SMB marking the contact between the northern Bundelkhand and southern Bastar Cratons in the Precambrian of central India. This narrow, 15 km wide, NE–SW to ENE–WSW trending gneiss dominated belt is in tectonic contact with the Sausar supracrustals in the SMB. The continuation of the granulite belt further west-southwestwards (from Bhandara) is uncertain as the area is under thick alluvial cover. East-northeastwards, granulite lithologies have been traced up to southeast of Balaghat and further in the same direction, presence of two-pyroxene granulite has been reported from the Ratanpur area. The above account indicates the regional extent of the granulite belt.

The contact between the granulite belt and the Sausar supracrustals is tectonic in nature. Though the lithologies of the granulite belt share later deformation events that have affected the Sausar supracrustals, they are characteristically different in other aspects from the latter. The Sausar supracrustals (without the Tirodi gneiss component) from the data available, show peak metamorphic condition only up to sillimanite grade without involving formation of a melt phase. The lithologies of the granulite belt, on the other hand, show, as documented in the present study, a high grade metamorphism under granulite facies and reaction relations suggest the polyphase nature of metamorphism. The high temperature ductile shears found in the granulite lithology are also absent from those of the Sausar supracrustals. All these point to the antiquity of the granulite facies protoliths as compared to Sausar supracrustals. Bhowmik and Pal (2000) from their study, have corroborated the present findings, and have indicated that the BBG granulites record two episodes of pre-Sausar metamorphism; an early high-T, moderate P metamorphism followed by an episode of cooling, showing IBC P-T-t path of evolution.

A sequence of metapelites including Al- and Mg-Al rich compositions is exposed discontinuously all along the eastern margin of the Sakoli

belt (figure 1). This sequence includes cordierite-K-feldspar—sillimanite—plagioclase—quartz—garnet; cordierite—gedrite-garnet—hornblende—plagioclase; gedrite-cordierite—plagioclase and quartz—sillimanite—kyanite-corundum-cordierite mineral parageneses, which are indicative of upper amphibolite facies metamorphic conditions. These rocks are closely interbanded with granitoid leucosomes and migmatitic gneiss containing garnetiferous amphibolite restites. It is a moot point if these supracrustals represent protolith of the lithologies occurring in the granulite belt, as, continuation of lithologies from these areas to the granulite belt could not be traced. If such a correlation is tenable, then the protoliths of the BBG belt would form a part of the Bastar Craton.

The BBG belt has been interpreted by Jain *et al* (1991, 1995) to represent exhumed oceanic crust of the northerly Bundelkhand protocontinent (with the Bundelkhand area as the nucleus) that was subducted below the southerly Deccan protocontinent (Bhandara or Central Indian Craton; Bastar Craton as referred to in this study) during a Palaeoproterozoic continent-continent collision event. These authors also considered the Sausar supracrustals (including the Tirodi gneiss) as representing the marginal basin of the northern (Bundelkhand) protocontinent. They then interpreted the BBG belt to be a suture zone. The present study has however shown that the magmatic rocks within the BBG belt are intra-plate (continental) rather than being plate margin or oceanic derivatives; the ultramafic-mafic association in the belt does not represent relict ophiolites; and evidences for deep sea sedimentary protoliths are not present, (Platformal) quartzite-K-pelite-BIF association in fact being the characteristic supracrustal association in the belt. It has also been shown that the two-pyroxene granulites in the BBG belt represent continental tholeiitic magma additions to the crust and can not be taken as evidence for exhumed oceanic crust. Additionally, presence of supracrustals similar to those in the BBG belt occurring in the area on the eastern margin of the Sakoli belt as mentioned earlier also goes against the hypothesis of Jain *et al* (1991, 1995).

Available geochronological data indicate an Rb-Sr whole-rock isochron age of 1525 ± 70 Ma from the Tirodi gneiss (Sarkar *et al* 1986) and a Rb-Sr whole rock isochron age of more than 2200 Ma for Amgaon gneiss (Sarkar *et al* 1981). A tentative retrogression age of 1300 Ma from hornblende in the two-pyroxene granulite from BBG belt through Ar/Ar method has been quoted in Yedekar and Jain (1995- from unpublished NSA, USA data). A younger age of 860 Ma from K-Ar systematics for the Tirodi gneiss has also been obtained (Sarkar *et al* 1967). Recently, a cooling age of 980 Ma from Ar/Ar systematics for Mn minerals in the Sausar supracrustals has been obtained by Lippolt and Hautmann (1994). As the Tirodi gneiss is considered to be older to the Sausar (Narayanaswamy *et al* 1963), it is possible that the younger ages mentioned above may be directly related to the evolution of the Sausar supracrustals. It is shown from this study that the lithologies in the BBG belt show both older and higher degree of (and polycyclic) metamorphism than the Sausar supracrustals. The continent-continent collision model invoked by Jain *et al* (1991, 1995) involves evolution of both the lithologies of the BBG belt and the Sausar supracrustals in one event. It is very unlikely to be so from data and interpretation presented in this work.

Sm-Nd dating of the charnockite and two-pyroxene granulite from the BBG belt recently has yielded two sets of dates at 2672 ± 54 Ma and 1416 ± 59 Ma, as well as Rb-Sr date of 1380 ± 28 Ma (Abhijit Roy, pers. comm.). The older, Archaean age, is interpreted to represent the first attained prograde granulite grade metamorphism in the BBG belt with charnockites retaining the early peak metamorphic assemblage of Grt (porphyro blast) +Opx+Pl. This was followed by the younger age representing the second granulite metamorphism, as seen from the development of coronal garnet (cooling texture) in the two-pyroxene granulite during Mesoproterozoic. It is postulated that, postdating the second event, the granulites were exhumed and thrust over the basement gneisses along the southern shear zone of the BBG belt, though it has not been possible to work out the exact timing of this shearing and exhumation event. This was followed by the development of Sausar belt in the north during terminal Mesoproterozoic. Sausar orogeny is the most pervasive and widespread in CITZ, imprints of which are recorded in all the pre-existing rocks. The penetrative foliation defined by amphibole in rocks of the BBG belt represents the imprints of much younger Sausar orogenic event. The development of the northern shear zone in the BBG belt thus coincides with the Sausar tectonothermal event with the development of amphibolite facies assemblages superposed on granulites. This corresponds with Rb-Sr ages of 800 ± 16 Ma in charnockites and 973 ± 63 Ma in mafic granulites (Abhijit Roy, pers. comm.).

It is thus concluded that the BBG belt most likely represents a part of the Bastar Craton, the gneiss-supracrustals sequence of which underwent polycyclic prograde granulite metamorphism prior to the evolution of the Sausar supracrustals. The granulite event in the more southerly Bhopalpatnam granulite belt in the southwestern part of the Bastar Craton, as can be judged from its cor-

relation with the Karimnagar belt, occurred at 2600 Ma (Rajesham *et al* 1993). The older Sm-Nd age of 2672 ± 54 Ma for charnockite in the BBG belt may be correlated with this event as representing a peak-metamorphic event within the BBG belt. It is not known if the post-peak Sm-Nd (also granulite facies) age of 1416 ± 59 Ma and Rb-Sr age of 1380 ± 28 Ma in two-pyroxene granulites of the BBG belt can be correlated with the younger Eastern Ghat granulite event at 1400–1600 Ma.

Acknowledgement

This paper is published with the kind permission of the Director General, Geological Survey of India. Comments by Dr. Samarendra Bhattachayya, Indian Statistical Institute and two anonymous reviewers have greatly helped in improving the quality of the paper.

References

Anderson J L and Bender E E 1989 Nature and origin of proterozoic A-type granite magmatism in southwestern U.S.A.; *Lithos* **23** 19–52

Barker F 1979 Trondhjemite: Definition, environment and hypotheses of origin. In *Trondhjemite, Dacites and related rocks*, (ed) F Barker: (Amsterdam: Elsevier), pp.1–12

Bhowmik S K, Pal T, Roy A and Pant N C 1999 Evidence for pre-grenvillian high-pressure granulite metamorphism from the northern margin of the sausar mobile belt in central India; *J.Geol. Soc. India* **53** 385–399

Bhowmik S K and Pal T 2000 Petrotectonic implication of the granulite suite north of the Sausar mobile belt in the overall tectonothermal evolution of the Central Indian Mobile Belt; GSI progress Report (Unpub), 82

Bohlen S R 1987 Pressure-temperature-time paths and a tectonic model for the evolution of granulites; *J.Geol.* **95** 617–632

Chappel B W and White A J R 1974 Two contrasting granite types; *Pacific Geology* **8** 173–174

Green D H and Ringwood A E 1967 An experimental investigation into the gabbro to eclogite transformation and its petrological applications; *Geochem. Cosm. Acta.* **31** 767–833

Harley S L 1992 Proterozoic granulite terranes; Chapter **8** In: *Proterozoic crustal evolution*, (ed) K Condie (Amsterdam: Elsevier), pp 301–359

Harley S L 1989 The origins of granulites: a metamorphic perspective; *Geol. Mag.* **126** 215–247

Harley S L and Fitzsimons J C W 1995 High-grade metamorphism and deformation in the Prydz Bay Region, East Antarctica: terranes, events and regional correlations, India and Antarctica during the Precambrian; *Mem. Geol. Soc. India* **34** 73–100

Huin A K, Chattopadhyay A and Khan A S 1998 A reappraisal of stratigraphy and structure of the Sausar mobile belt around Deolapar-Pauni-Manegaon area, Nagpur district, Maharashtra, India; In: *International Seminar on Precambrian crust in eastern and central India*, UNESCO-IUGS-IGCP-368, Bhubaneswar, India, Abstracts. Pp. 38–40

Irvine T N and Baragar W R A 1971 A guide to the chemical classification of the common volcanic rocks; *Can.J.Earth Sci.* **8** 523–548

Jensen L S and Pyke D R 1982 Komatiites in the Ontario portion of the Abitibi belt In: *Komatiites. Geol.* (eds) N T Arndt and E G Nesbitt (Allen and Unwin, London) Pp. 147–157

Jain S C, Yedekar D B and Nair K K K 1991 Central Indian Shear zone : A major precambrian crustal boundary; *J. Geol. Soc. India* **37** 521–531

Jain S C, Nair K K K and Yedekar D B 1995 Geology of the Son-Narmada-Tapti lineament zone in central India; In: *Geoscientific studies of the Son-Narmada-Tapti lineament zone.* Sp. Pub. GSI **10** 1–154

Khan A S, Huin A K and Chattopadhyay A 1998 Specialized thematic mapping in Sausar Fold Belt in Deolapar-Pauni area, Nagpur and Bhandara districts, Maharashtra, for elucidation of stratigraphy, structure, metamorphic history and tectonics; *Records Geol. Surv. India* **131** part 6 31–35

Khan A S, Huin A K and Chattopadhyay A 1999 Specialized thematic mapping in Sausar Fold Belt in Manegaon-Karwahi, Totladoh-Kirangi, Sarra and Susurdoh-Sitekasa area, Nagpur and Bhandara districts, Maharashtra, for elucidation of stratigraphy, structure, metamorphic history and tectonics; *Records Geol. Surv. India* **132** part 6 31–35

Lippolt H J and Hautmann S 1994 $^{40}Ar/^{39}Ar$ ages of Precambrian manganese ore minerals from Sweden, India and Morocco; *Mineralium Deposita* **18** 195–215

Mishra V P, Pushkar Singh and Dutta N K 1988 Stratigraphy, structure and metamorphic history of Bastar district, M.P; *Rec. Geol. Surv. India* **117** 1–26

Mohabey N K and Dekate Y G 1984 Variation in the properties of hornblende produced during progressive metamorphism of mafic rocks west-northwest of Bhandara, Maharashtra; Spec.pub. GSI **12** 391–400

Narayanaswamy S, Chakraborty S C, Vemban N A, Shukla K D, Subramanyam M R, Venkatesh V, Rao G V, Anandalwar M A and Nagarajaiah R A 1963 The Geology and manganese ore deposits of the manganese belts in Madhya Pradesh and adjoining areas of Maharashtra; *Geol. Soc. India. Bull. Ser. A* **22** 69 pp.

Narayanaswamy S and Venkatesh V 1971 The geology and manganese deposits of northern Bhandara district, Maharashtra, in Part IV of the Geology and Manganese ore deposits of the Manganese belt in Madhya Pradesh and adjoining parts of Maharashtra; *Bull. Geol. Surv. India Ser.* A **22** 183 pp.

Pearce T H, Gormann B E and Birkett T C 1975 The TiO_2 - K_2O - P_2O_5 diagram : a method of discriminating between oceanic and non-oceanic basalts; *Earth Planet. Sci. Lett.* **24** 419–426

Prakash Narasimha K N, Janardhan A S and Mishra V P 1996 Granulites of Bhopalpatnam and Kondagaon belts, Bastar Craton, M.P.: petrological and fluid inclusion studies; *J. S E Asian Sci.* **14** 221–229

Rajesham T, Bhaskar Rao Y J and Murti K S 1993 The Karimnagar granulite terrane – A new sapphirine bearing granite province, South India; *J. Geol. Soc. India* **41** 51–59

Rajurkar S T 1974 Report on the investigation for platinum in the hill mass between Chikalbori and Mohdura villages, in parts of Nagpur and Bhandara districts, Maharashtra State; *Unpub. Prog. Rep. GSI FS* **71-72** 14

Ramachandra H M, Mishra V P, Roy A and Dutta N K 1998 Evolution of the Bastar Craton – a critical review of gneiss-granitoids and supracrustal belts (Abs.) M S Krishnan Centenary Commemorative National Seminar, Calcutta, pp 144–150

Roy A, Ramachandra H M and Bandyopadhyay B 2000 Supracrustal belts and their significance in the crustal evolution of central India; *Geol. Surv. India. Spl. Pub* **55** 361–380

Sarkar S N, Gerling E K, Polkanov A A and Chukov F V 1967 Precambrian geochronology of Nagpur-Bhandara-Durg, India; *Geol. Mag.* **104** 525–549

Sarkar S N, Gopalan K and Trivedi J R 1981 New data on the geochronology of the Precambrians of the Bhandara-Durg, Central India; *Indian J. Earth Sci.* **8** 131–151

Sarkar S N, Trivedi J R and Gopalan K 1986 Rb-Sr whole rock and mineral isochron ages of the Tirodi gneiss, Sausar Group, Bhandara district, Maharashtra; *J. Geol. Soc. India* **27** 30–37

Wilson M 1989 *Igneous petrogenesis.* (London: Unwin Hyman)

Yardley B W D 1989 *An Introduction to Metamorphic Petrology.* (London: ELBS / Longman), 248 p.

Yedekar D B and Jain S C 1995 Geological studies along Seoni-Rajnandgaon transect, Madhya Pradesh and Maharashtra; *Rec. Geol. Surv. India* **128** 205–208